

## Interstellar Cosmic-ray Electron Spectrum from Synchrotron Radiation and direct Measurements

ELENA ORLANDO<sup>1,2</sup> AND ANDREW W. STRONG<sup>2</sup>

<sup>1</sup>*HEPL/KIPAC Stanford University*

<sup>2</sup>*Max-Planck-Institut für extraterrestrische Physik, Garching, Germany*

*eorlando@stanford.edu*

DOI: 10.7529/ICRC2011/V06/1161

**Abstract:** We use synchrotron radiation to constrain the low-energy local interstellar cosmic-ray electron spectrum (LIS), models of propagation of cosmic rays, solar modulation and the Galactic magnetic field. Surveys over a wide range of radio frequencies are used, including spectral index data. Some propagation models involving reacceleration are shown to be excluded by synchrotron data, and others have their injection index constrained. Implications for solar modulation are also presented.

**Keywords:** cosmic rays - synchrotron radiation - magnetic fields – radio data

### 1 Introduction

Fermi-LAT measured the electron spectrum from 7 GeV to 1 TeV, with unprecedented accuracy [1, 2]. Above 20 GeV the Fermi-LAT electron spectrum can be fitted with a simple power law with spectral index 3.04. More recently, PAMELA has measured the spectrum from 1 GeV to 625 GeV [10]. H.E.S.S. [3,4] and ATIC [5] have measured the spectrum to higher energies.

Direct measurements of cosmic-ray (CR) electrons at energy lower than a few GeV are affected by solar modulation that complicates their interpretation. During solar minimum, when the CR flux is maximum, measurements at lower energies are based on HEAT [6], CAPRICE94 [7] and AMS01 [8]. Below a few GeV the local interstellar electron spectrum cannot be measured and its determination is very uncertain. In [11], we exploit synchrotron radiation (from tens of MHz to tens of GHz), which probes interstellar electrons from 0.5 to 20 GeV for the typical Galactic magnetic field (hereafter B-field) of a few  $\mu\text{G}$ . It is used in conjunction with direct measurements to construct the local interstellar spectrum. At low energies this will finally allow an independent estimate of solar modulation for testing heliopheric propagation models.

We use the CR propagation code GALPROP [12,13,14] to generate interstellar spectra for various propagation scenarios. It is shown that some current models are ac-

tually excluded on the basis of the synchrotron data. Full details are given in our recent work [11]. A related analysis concentrating on the Galactic plane is given in [21].

### 2 Evidence of the break in the LIS

Many measurements show that the spectral index of the brightness temperature (intensity index + 2) of the synchrotron emission increases steadily from about 2.5 to 3.0 over the frequency range from tens of MHz to tens of GHz. A review of radio continuum surveys and their calibration is given in [15]. We listed some representative results from the literature on spectral indices in [11]. The most recent determination of the spectral index 45-408 MHz [16] gives 2.5-2.6, implying an ambient electron index of 2.0-2.2 for electrons below a few GeV. This completely excludes a continuation of the ambient electron index of 3.0-3.2 measured by Fermi-LAT  $>7$  GeV to lower energies. At the same time the synchrotron index  $> 1$  GHz has been found by many authors to be near 3, fully consistent with the measured ambient electron spectrum above a few GeV (ambient index 3.0-3.2 giving synchrotron index 3.0-3.1). Hence, independent of the propagation model, the primary electron spectrum must turn over below a few GeV, with an ambient index around 2.

### 3 Propagation models

We use GALPROP to generate synchrotron spectra for various propagation scenarios. A description of the GALPROP model can be found in [12] and references therein; in particular see [13, 14]. The code has been developed as described in [11] in order to model the synchrotron emission. Electrons and positrons lose energy by synchrotron radiation, and this is included in GALPROP self-consistently using the B total of the adopted model. Inverse Compton, bremsstrahlung and ionization energy losses are also included.

Propagation models based on cosmic-ray and gamma-ray data are tested against synchrotron data from 22 MHz to over 94 GHz. The radio surveys and the method used are described in [11].

We use the GALPROP models with parameters described in [17], to which we refer for details. These models are consistent with CR nuclei secondary-to-primary ratios. Only the electron injection spectrum and the B-field are varied here with respect to these models; these do not affect the validity of the propagation parameters.

In order to avoid absorption effects at low frequency, and free-free emission at higher frequencies, and to avoid effects of zero-level corrections and local emission, the analysis is restricted to regions out of the Galactic plane but avoiding the polar regions, and also avoiding the North Polar Spur. We use  $10^\circ < |b| < 45^\circ$ .

### 4 Galactic magnetic fields

In [18] only the random component of the magnetic field was present and was implemented in 2D in GALPROP with an exponential law. Since that work, many 3D models of the Galactic magnetic field have been implemented in GALPROP in order to calculate the synchrotron emission from the Galaxy. The regular B-field used in the present work is the model RING-ASS of [19] for the disk, based on rotation measures of extragalactic radio sources. This has typically  $B_{\text{reg}} = 2 \mu\text{G}$ . A toroidal halo field is also included as prescribed in [20], having a typical value of  $2 \mu\text{G}$ . We include the regular field in order to make our model compatible with current information, but in fact since it is much less than the random field, this is not critical to our study.

The magnitude of the B-field is a free parameter in this analysis, since while the regular component can be determined from rotation measures of pulsars and extragalactic sources, this is only a fraction of the total field. Our approach in [11] is to use the models for the regular component derived from RMs, combining these with a random field to be determined, and the latter is one of the results of our analysis. At 408 MHz and above, secondary leptons (above a few GeV) become less important for synchrotron and the relevant leptons are measured directly without much solar modulation, while at higher frequencies ( $>1$  GHz) free-free emission can start to enter. Our model for  $B_{\text{ran}}$  is therefore based on fits to the data at 408 MHz. The random field is modelled as a double

exponential in  $(R,z)$ , the free parameters being the two scale lengths (30 kpc in  $R$  and 4 kpc in  $z$ ) and the local B-field:  $B_{\text{ran}} = 7.5 \mu\text{G}$ .

## 5 Results

### 5.1 Diffuse model: a break on the injection spectrum

We consider first a ‘pure diffusion’ model, with a halo height of 4 kpc. The complete set of GALPROP parameters are given in [17], model z04LMPDS. The electron injection spectrum breaks at 4 GeV and 50 GeV, with indices 1.6/2.5/2.2. The break at 50 GeV is to fit the Fermi-LAT low-energy upturn, the break at 4 GeV to fit low-frequency synchrotron. We first show the effect of varying the low-energy ( $<4$  GeV) electron injection index, from 1.3 to 2.5. Fig 1 shows the interstellar electron spectra for these models, and also for various modulation levels using the force-field approximation. It is clear that the electron data alone cannot distinguish the models due to the modulation uncertainty, so that the synchrotron constraints are essential.

Fig 2 shows that a low-energy primary electron injection index of 2.0 is too high and excluded by the synchrotron data. The best fit is actually for an injection index around 1.3 (see Fig 2). Low frequencies (below 100 MHz) are dominated by leptons with energies less than 4 GeV. Secondary leptons produce one third of the observed low-frequency intensity and hence make determination of the primary spectrum more difficult.

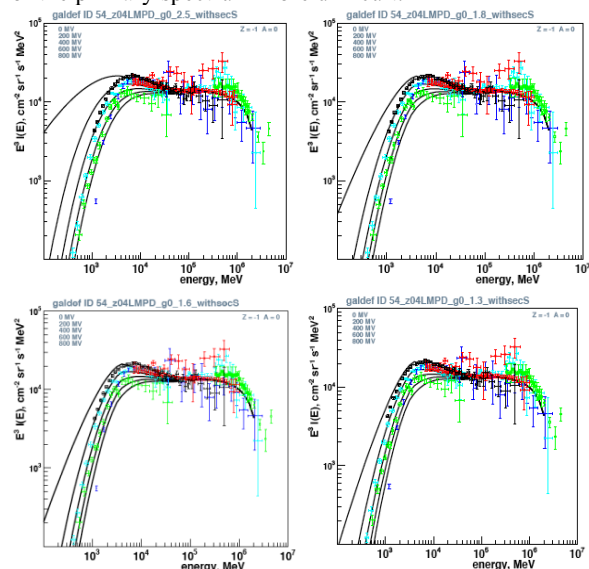


Figure 1. Electron spectra for pure diffusion model, low-energy electron injection index 2.5, 1.8, 1.6 and 1.3 for modulation 0, 200, 400, 600 and 800 MV. Cyan open circles: AMS01; green crosses and filled circles: CAPRICE; blue squares: HEAT; red filled circles: Fermi-LAT; black filled circles: PAMELA; blue triangles: SARIKU; red crosses: BETS, PPT-BETS.

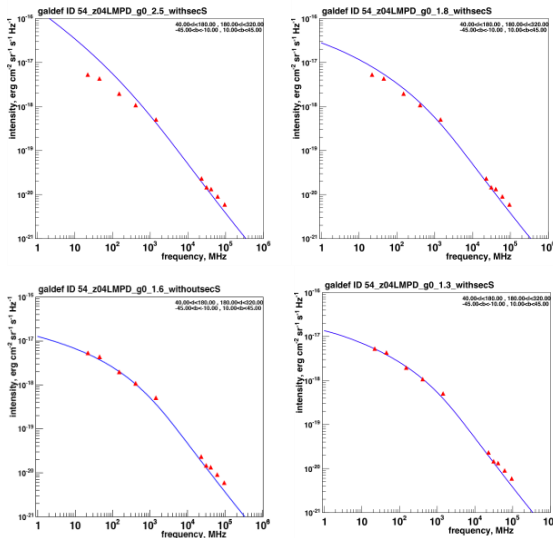


Figure 2. Synchrotron spectra for pure diffusion model with low-energy electron injection index (left to right, top to bottom) 2.0, 1.8, 1.6 and 1.3. Including secondary leptons. Data are described in [11].

## 5.2 Reacceleration model: challenged by synchrotron

We now consider a reacceleration model, also with halo height 4 kpc. The complete set of GALPROP parameters are given in [17], model z04LMS; the injection spectral index above 4 GeV has been reduced from 2.42 in that model to 2.3 to better fit the Fermi electron data above 20 GeV. It is clear that this particular reacceleration model is not consistent with the observed synchrotron spectrum, since the sum of primary and secondary leptons produces too high intensities at low frequencies (see Fig. 3). It could be adjusted by making the low-energy injection index smaller, as for the pure diffusion model. However a large part of the excess comes from the secondary leptons which have a large peak due to reacceleration which makes them equal to primary electrons around 1 GeV, and which cannot be adjusted very much in this model (Fig. 3); this peak is not present in the pure diffusion model. Only if the secondaries are removed does the synchrotron give a good fit, while the secondary production is certainly present. This does not mean that reacceleration models are excluded by this study, but it does pose a challenge for future work on such models.

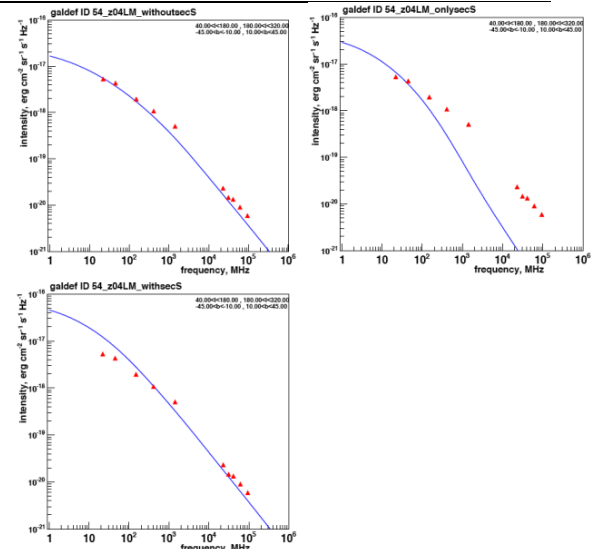


Figure 3. Synchrotron spectra for diffusive reacceleration model with primary low-energy electron injection index 1.6. Synchrotron from primary electrons (upper left), secondary leptons (upper right) and total (lower). Data are described in [11].

## 6 Conclusions

Our main conclusion is that the interstellar CR electron spectrum must turn over rather sharply below a few GeV. This result is independent of how the spectrum is formed by injection and propagation. However it seems difficult to explain as a propagation effect, so probably reflects the electron injection spectrum from the sources. The low-energy falloff in the directly measured electrons, normally attributed mainly to modulation, may instead reflect mainly the interstellar spectrum. The (model-dependent) injection index implied for the primary electrons is 1.3-1.6 below a few GeV, and 2.1-2.3 at higher energies. This suggests less solar modulation than usually assumed. The standard reacceleration model is not consistent with the observed synchrotron spectrum, since the total from primary and secondary leptons exceeds the measured synchrotron at low frequencies. While not excluding reacceleration models, it does pose a challenge to be addressed in future.

## 7 References

- [1] Abdo, A. A., Ackermann, M., Ajello, M., et al. 2009b, *Physical Review Letters*, 102, 181101
- [2] Ackermann, M., Ajello, M., Atwood, W. B., et al. 2010, *Phys. Rev. D*, 82, 092004
- [3] Aharonian, F., Akhperjanian, A. G., Anton, G., et al. 2009, *A&A*, 508, 561
- [4] Aharonian, F., Akhperjanian, A. G., Barres de Almeida, U., et al. 2008, *Physical Review Letters*, 101, 261104
- [5] Chang, J., Adams, J. H., Ahn, H. S., et al. 2008, *Nature*, 456, 362
- [6] DuVernois, M. A., Barwick, S. W., Beatty, J. J., et al. 2001, *ApJ*, 559, 296
- [7] Boezio, M., Carlson, P., Francke, T., et al. 2000, *ApJ*, 532, 653
- [8] AMS Collaboration, Aguilar, M., Alcaraz, J., et al. 2002, *Phys. Rep.*, 366, 331
- [9] Adriani, O., Barbarino, G. C., Bazilevskaya, G. A., et al. 2009, *Nature*, 458, 607
- [10] Adriani, O., Barbarino, G. C., Bazilevskaya, G. A., et al. 2011, *Physical Review Letters*, 106, 201101
- [11] Strong, A. W., Orlando, E., & Jaffe, T. R. 2011, arXiv:1108.4822
- [12] Strong, A. W., Moskalenko, I. V., & Ptuskin, V. S. 2007, *Annual Review of Nuclear and Particle Science*, 57, 285
- [13] Strong, A. W. & Moskalenko, I. V. 1998, *ApJ*, 509, 212
- [14] Moskalenko, I. V., & Strong, A. W. 1998, *ApJ*, 493, 694
- [15] Reich, W. & Reich, P. 2009, in *IAU Symposium*, Vol. 259, *IAU Symposium*, 603–612
- [16] Guzman, A. E., May, J., Alvarez, H., & Maeda, K. 2011, *A&A*, 525, A138
- [17] Strong, A. W. 2011, arXiv:1101.1381
- [18] Strong, A. W., Moskalenko, I. V., & Reimer, O. 2000, *ApJ*, 537, 763
- [19] Sun, X. & Reich, W. 2010, *Research in Astronomy and Astrophysics*, 10, 1287
- [20] Sun, X. H., Reich, W., Waelkens, A., & Enßlin, T. A. 2008, *A&A*, 477, 573
- [21] Jaffe, T. R., Banday, A. J., Leahy, J. P., Leach, S., & Strong, A. W. 2011, *MNRAS*, in press, arXiv:1105.5885